



Multivariate resting-state functional connectivity predicts response to cognitive behavioral therapy in obsessive–compulsive disorder

Nicco Reggente^{a,1}, Teena D. Moody^b, Francesca Morfini^b, Courtney Sheen^b, Jesse Rissman^{a,b}, Joseph O’Neill^c, and Jamie D. Feusner^b

^aDepartment of Psychology, University of California, Los Angeles, CA 90095; ^bDepartment of Psychiatry and Biobehavioral Sciences, David Geffen School of Medicine at University of California, Los Angeles, CA 90095; and ^cDivision of Child and Adolescent Psychiatry, David Geffen School of Medicine at University of California, Los Angeles, CA 90095

Edited by Cameron Carter, University of California, Davis, CA, and accepted by Editorial Board Member Marlene Behrmann January 10, 2018 (received for review September 21, 2017)

Cognitive behavioral therapy (CBT) is an effective treatment for many with obsessive–compulsive disorder (OCD). However, response varies considerably among individuals. Attaining a means to predict an individual’s potential response would permit clinicians to more prudently allocate resources for this often stressful and time-consuming treatment. We collected resting-state functional magnetic resonance imaging from adults with OCD before and after 4 weeks of intensive daily CBT. We leveraged machine learning with cross-validation to assess the power of functional connectivity (FC) patterns to predict individual posttreatment OCD symptom severity. Pretreatment FC patterns within the default mode network and visual network significantly predicted post-treatment OCD severity, explaining up to 67% of the variance. These networks were stronger predictors than pretreatment clinical scores. Results have clinical implications for developing personalized medicine approaches to identifying individual OCD patients who will maximally benefit from intensive CBT.

OCD | CBT | resting state | functional connectivity | machine learning

Obsessive–compulsive disorder (OCD) is characterized by recurrent intrusive thoughts (obsessions) and/or repetitive behaviors (compulsions) (1). OCD has a lifetime prevalence of ~1–2% worldwide (2) and is associated with poor quality of life, functional impairment, and increased use of health care services (3).

Cognitive behavioral therapy (CBT), including intensive CBT, shows moderate-to-high effectiveness for OCD (4, 5). However, response varies significantly among individuals (6). In addition, specialized CBT is expensive, stressful, and time-consuming and often has limited availability (7). This underscores the importance of developing reliable predictors of response to treatment to aid clinical decision-making.

Many studies have identified psychometric and demographic features that correlate with treatment response (8) but, unfortunately, do not consistently predict outcome (9). Neuroimaging biomarkers have recently shown promise at predicting response to treatment (10). However, only one small study using symptom provocation functional magnetic resonance imaging (fMRI) (11) and one study of brain connectivity using resting-state fMRI (12) have drawn correlations between baseline neural measures and subsequent response to CBT. Feusner et al. (13) previously found that pretreatment brain network small-worldness, a graph theory measure derived from resting-state fMRI, was associated with the trajectory of OCD symptoms up to 12 mo after intensive CBT and that small-worldness increased pre- to post-CBT.

Another OCD study (14)—this time of serotonin reuptake inhibitor (SRI) treatment—found significant pretreatment to posttreatment changes in network connectivity in the frontoparietal, cinguloopercular, somatosensory–motor, and visual networks. Although this study also did not focus on predicting response to treatment, the observation that connectivity changed

with treatment in these networks provides a rationale for examining their predictive ability in relationship to clinical outcomes.

No studies to date have applied multivariate approaches to investigate changes in brain connectivity pretreatment to post-treatment, to predict treatment outcome, or to predict symptom trajectory after treatment. Multivariate analyses of brain connectivity offer advantages of simultaneously capturing patterns involving multiple connections, likely better reflecting the complexity of brain networks than standard univariate approaches. Multivariate pattern recognition analyses have proven to be more sensitive than conventional univariate analyses in assessing the link between neuroimaging and behavioral variables to predict the presence or absence of other brain disorders (15, 16).

Here we utilized a multivariate approach to explore pretreatment network connectivity patterns that might presage posttreatment symptom severity. Multivariate analysis was applied to whole-brain resting-state fMRI acquired before and after 4 wk of intensive CBT and before and after a waitlist control condition. Our search were data-driven but restricted to networks where connectivity patterns had previously been found to change with treatment (14) because networks that reorganize during treatment might also be predictive of treatment outcome. These included the above-mentioned frontoparietal,

Significance

The ability to predict an individual’s potential response to treatment would permit clinicians to more prudently allocate resources that support cognitive behavioral therapy for obsessive–compulsive disorder (OCD), an often stressful and time-consuming treatment. The current study lays important groundwork for an exciting advance toward personalized medicine in psychiatry that up to this point has eluded the field. This study marks a success in using multivariate pattern recognition to identify neurobiological predictors of treatment response. In addition, it advances knowledge of the neurophysiology of OCD and of mechanistic processes involved in the therapeutic response, which could be used to refine existing treatments or to develop novel treatments based on identified potential brain targets.

Author contributions: N.R., T.D.M., C.S., J.O., and J.D.F. designed research; N.R., T.D.M., F.M., C.S., and J.D.F. performed research; N.R., T.D.M., J.R., and J.D.F. contributed new reagents/analytic tools; N.R., T.D.M., and F.M. analyzed data; and N.R., T.D.M., F.M., J.R., J.O., and J.D.F. wrote the paper.

The authors declare no conflict of interest.

This article is a PNAS Direct Submission. C.C. is a guest editor invited by the Editorial Board.

Published under the PNAS license.

¹To whom correspondence should be addressed. Email: nreggente@psych.ucla.edu.

This article contains supporting information online at www.pnas.org/lookup/suppl/doi:10.1073/pnas.1716686115/-DCSupplemental.

cinguloopercular, somatosensory–motor, and visual networks. To these we added the default mode network (DMN) (17–20) and the dorsal and ventral attention networks (21), where previous studies found abnormal connectivity in OCD. We additionally included the subcortical network given the well-known cortico-striato-thalamo-cortical hyperactivity in OCD, including (but not limited to) caudate and putamen, which might be affected by CBT (22, 23). All network-defined regions of interest (ROIs) were derived from Power et al. (24), who parcellated the brain into functional networks based on resting-state connectivity data and metaanalysis of task fMRI studies (24).

Finally, the amygdala, compared with many other brain regions, has shown particular value in predicting response to CBT for OCD (11, 12) and has frequently exhibited abnormalities in OCD involving blood oxygenation level-dependent (BOLD) activation (25–29) and/or functional connectivity (21, 30–32). Therefore, we performed additional analyses in which we added bilateral amygdala ROIs from the Harvard Oxford Atlas to the list of ROIs within each network.

Methods and Materials

Recruitment and Assessment. We recruited participants from University of California, Los Angeles (UCLA), clinics and through flyers and Internet advertisements. All experimental procedures were approved by the UCLA Institutional Review Board, and all participants provided written informed consent before participation. OCD diagnosis was established through interviews by one author (J.D.F.), who has clinical experience with this population. Primary OCD and comorbid diagnoses were determined using the *Anxiety Disorders Interview Schedule for DSM–IV–Mini (ADIS–IV–Mini)* (33). OCD participants were eligible if they scored at least a 16 on the Yale–Brown Obsessive Compulsive Scale (YBOCS) (34). Participants could be unmedicated or taking SRIs if there were no changes in medication within 12 wk of enrollment. For detailed inclusion/exclusion criteria, please see [Supporting Information](#).

Psychometric Evaluations. Primary outcome was the YBOCS. Secondary measures pretreatment to posttreatment included the Hamilton Anxiety Scale (HAMA) (35) and the Montgomery–Åsberg Depression Rating Scale (MADRS) (36). General functionality and social/occupational performance was rated with the Global Assessment Scale (GAS) (37). An independent evaluator, not involved in treatment or assessments, administered psychometric instruments.

Treatment. All 42 OCD participants underwent manualized (38) exposure and response prevention (ERP)-based intensive CBT. Individual treatment plans consisted of 90-min sessions, 5 d per week, for 4 wk, as previously described (13). Approximately half ($n = 21$) were randomized to a 4-wk minimal-contact waitlist-first condition followed by treatment.

fMRI Acquisition and Processing. Whole-brain BOLD fMRI was collected using a 7-min echo-planar imaging sequence [3T Siemens Trio; 12-channel head coil; repetition time/echo time (TR/TE) = 2,000/25 ms; flip 78°; voxels 3 mm³; 1-mm gap; 35 axial slices; field of view 195 mm anterior to posterior, 195 mm right-left, 139 mm foot to head] within 1 wk before treatment and within 1 wk after treatment. Those randomized to the waitlist-first condition were also scanned within 1 wk before they started the 4-wk waitlist, as well as before and after treatment. Participants were instructed to rest with eyes closed and not to sleep. T1-weighted structural MRI [axial magnetization-prepared rapid gradient-Echo (MPRAGE), TR/TE = 1,900/3.26 ms, voxels 1 mm³] was coacquired for registration.

Functional data were preprocessed without spatial smoothing using the FMRI Software Library 5.0.4 (<https://fsl.fmrib.ox.ac.uk/fsl/fslwiki>). Data were motion-corrected using FMRIB's Linear Image Registration Tool for Motion Correction (MCFLIRT) and band-pass filtered (0.009–0.08 Hz). Seven and 12 degrees-of-freedom transforms were used to register functional images to MPRAGE and to Montreal Neurological Institute space, respectively, and images were resampled to 2 mm³. Nuisance covariates included global signal and cerebrospinal fluid signal (along with their first derivatives) as well as 6 head motion parameters, for a total of 10 parameters; these were removed by linear regression. Motion was assessed using DVARS (root-mean-squared change in volume-to-volume BOLD signal) (39) and framewise displacement (FD) (39, 40) to compare pre- vs. post-CBT and to exclude those with DVARS > 2 SD above the mean and those with FD > 0.3 in either session. Two

participants' data were excluded due to excessive head motion (FD > 0.3 for one and DVARS > 2 SD in another), resulting in a total of 42 participants for our functional analyses. There were no significant differences in motion as measured by DVARS pre-CBT (29.1 ± 4.4) vs. post-CBT (28.5 ± 4.7) ($P = 0.44$, paired t test). Nor were there significant differences in motion as measured by FD pre-CBT (0.13 ± 0.06) vs. post-CBT (0.13 ± 0.05) ($P = 0.59$, paired t test). Before functional connectivity-based analyses, each voxel's time course was z-scored.

Functional Connectivity Matrix Construction. Mean BOLD time courses were extracted from the average activity across voxels in 196 spherical ROIs with 5-mm radius (24). These belonged to the aforementioned cinguloopercular ($n = 14$ ROIs), frontoparietal ($n = 25$), ventral attention ($n = 9$), dorsal attention ($n = 11$), visual ($n = 31$), somatosensory–motor ($n = 35$), default mode ($n = 58$), and subcortical ($n = 13$) networks of interest (14, 17–19, 22, 23, 41–45). Matrices of correlation coefficients were created for each participant by computing pairwise correlations of each ROI's mean BOLD time course with that of all other ROIs (Fig. 1A). For additional analyses, bilateral amygdala ROIs from the Harvard Oxford Cortical and Subcortical Structural Atlas (<https://fsl.fmrib.ox.ac.uk/fsl/fslwiki/Atlases>) were thresholded at 50% population probability and included in the list of ROIs within each network.

Feature Selection. For each participant, features included the functional connectivity (FC) values between the ROIs within each network, pretreatment YBOCS score, and a binary medication variable indicating whether or not psychotropics were being taken at time of scan. We included YBOCS and medication as features because they represent potentially informative, and readily obtained, a priori clinical information that might add predictive value. Thus, each participant's feature set consisted of $n(n-1)/2 + 2$ features, n being the number of ROIs in the network of interest (Fig. 1B).

Machine Learning Multivariate Regression Analyses. To control for variations in age, sex, illness duration, and IQ [Wechsler Abbreviated Scales of Intelligence (WASI) scores] across participants, each feature was iteratively submitted to multiple linear regression with the aforementioned variables as predictors. The residuals were used as the new features.

We built a least absolute shrinkage and selection operator [LASSO (46)] regression model whose regularization parameter was optimized using the least angle regression (LARS) algorithm (47) on an $N - 1$ cross-validation that maximized the Pearson correlation between actual and predicted post-treatment YBOCS scores. To minimize overfitting, we used these optimized model parameters in an $N - 10$ cross-validation, where a random subset of 10 participants (~25%) were left out and the model was trained on the remaining participants. For our 42 participants, this yielded four folds, plus an additional fold of the cross-validation that left out two participants. Using the model's intercept term and outcome beta values as coefficients for each feature value, we used the weighted sum of each left-out participant's features to obtain predicted behavioral measures of interest (\hat{Y}). After the five folds, whereby each participant was left out exactly once, we correlated the array of predicted values (\hat{Y}) with the actual values (Y), yielding Pearson's R and R^2 —a measure of our model's feature-dependent ability to capture the behavioral variance across participants. We repeated this five-fold cross-validation 10 times and averaged the R values to converge on a true estimate of our test statistic independent of which participants were randomly included in each fold. We also report the RMSE [$\sqrt{\frac{1}{N} \sum_{i=1}^N (\hat{Y}_i - Y_i)^2}$] values averaged across the 10 iterations.

Machine Learning Classification Analyses. For a series of follow-up analyses, we used the same feature sets to train a linear nu-support vector classifier (nu-SVC, $c = 1$; ref. 48). For each analysis of interest, we used a leave-10-participants-out cross-validation approach that balanced training class examples by randomly removing examples from the overrepresented class. We ran this cross-validation 10 times and report the average accuracy values.

Significance Testing. We first report the significance of the correlation coefficients by comparing the R -value to a Student's t distribution (p_t). To account for multiple comparisons across our different networks of interest, we used a Bonferroni-corrected significance level of $p \leq .006$ (0.05/8 networks). To confirm that our classification scheme was not subject to bias and was immune to parametric assumption violations, we also compared significant R values ($p_t \leq .006$) to an empirical null distribution created with a bootstrap procedure (p_{bs}). See [SI Methods](#).

For all SVM analyses, significance was determined by the binomial inverse of the cumulative distribution function to identify the smallest number of

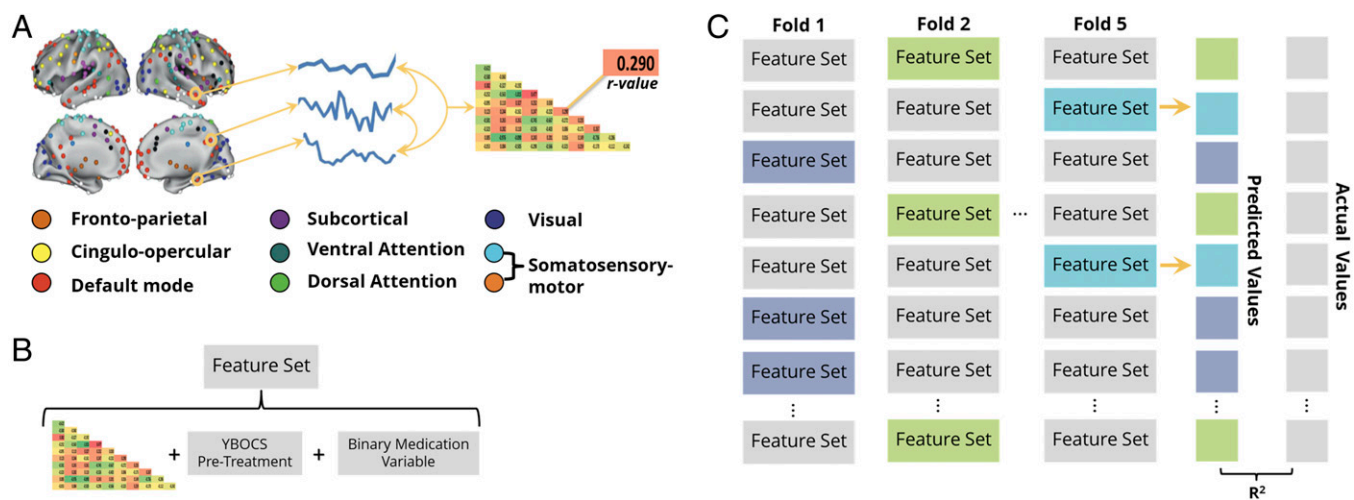


Fig. 1. (A) The average resting-state activity within ROIs from eight functional brain networks defined by Power et al. (24) was used to create a mean BOLD time course. A pairwise Pearson correlation of these time courses resulted in a functional connectivity (FC) matrix specific to each network. (B) The lower diagonal of each participant's network-specific FC matrix was concatenated with the participant's pretreatment YBOCS score and a binary variable indicating whether or not the participant was on medication to create a feature set for that participant. (C) A LASSO regression model was trained on $n - 10$ participants' feature sets and their associated posttreatment YBOCS values and used to predict each of the left-out participant's posttreatment YBOCS scores. Left-out participants are denoted as shaded feature sets (only three shown here due to space constraints). This process was repeated until all participants had been left out in a fold of the cross-validation and had been assigned a predicted posttreatment YBOCS (\hat{Y}). We correlated the array of predicted values (\hat{Y}) with the actual values (Y), yielding Pearson's R and R^2 , a measure of our model's feature-dependent ability to capture the behavioral variance across participants. Note that due to our participant sample size ($n = 42$), one fold of the cross-validation left out two participants, exemplified in fold 5.

correct classifications of the total number of classifications (number of participants raised to the power of the number of groups in the classification), where the distribution was centered around the chance value by randomly shuffling the labels before classification (49).

Top Connections. For each fold of the cross-validation, the betas used to predict the left-out participants were stored. The average beta for each FC feature was calculated and sorted as a function of magnitude. For visualization purposes, the top 5% of connections in each network that reached significance can be seen in Figs. S1 and S2.

Results

Participants. Fifty-one right-handed adults ages 18–60 with the *Diagnostic and Statistical Manual of Mental Disorders, 4th edition (DSM-IV)* (50) OCD were enrolled. Four waitlist-first participants withdrew before completing waitlist, and one was withdrawn due to medication protocol violation. The study physician withdrew two treatment-first participants, and two completed the study but had inadequate fMRI data due to head motion. Ultimately, data from 42 OCD participants were analyzed. Thirteen were medicated: six with fluoxetine, one with fluvoxamine, two with escitalopram, and three with sertraline. Twenty-nine had one or more comorbid psychiatric diagnoses (Table 1 and Table S1).

Symptom Changes. YBOCS improved pre- to post-CBT in 41 of 42 OCD participants [pre-CBT mean: 24.6 ± 4.7 , post-CBT: 15.0 ± 5.3 ; improvement 9.6 ± 5.9 (39.0%), 95% CI, 8.8–11.3; $t_{41} = 10.5$, $P < 0.001$] (Table 1). Prewaitlist to postwaitlist, there was little change in YBOCS [prewaitlist: 25.8 ± 4.9 , postwaitlist 25.0 ± 5.4 ; 0.90 ± 3.1 (3.2%) improvement: $t_{41} = 1.21$, $P = 0.24$]. Pretreatment and posttreatment YBOCS scores were only moderately associated ($R^2 = 0.095$, $P = 0.047$).

Functional Connectivity. Two of the pretreatment FC feature sets strongly and reliably predicted a participant's posttreatment YBOCS (Fig. 2). When the DMN's pretreatment FC values were used in the feature set, the classification was most powerful, capturing 67% of the variance in posttreatment YBOCS ($R^2 = 0.67$; RMSE = 3.32; $p_t < 0.001$; $p_{bs} < 0.001$). Pretreatment

FC within the visual network also accounted for significant variance ($R^2 = 0.51$; RMSE = 3.69; $p_t < 0.001$; $p_{bs} < 0.001$). No other networks reached statistical significance (Table 2).

For networks whose pretreatment FC was informative when predicting posttreatment YBOCS, we examined the effect of including bilateral amygdala ROIs with each network. Neither the DMN nor the visual network saw an increase in predictive ability from the inclusion of the amygdala. To determine the effect of the additional features (pretreatment YBOCS and the binary medication variable), we reran the LASSO cross-validation without these features (relying only on FC patterns within the networks of interest) and observed moderately higher predictive

Table 1. Demographic and psychometric characteristics of the sample ($N = 42$)

Characteristic	Value	SD	P value
Female/male	22/20		
Age	32.4	9.9	
Education, y	15.6	2.4	
WASI IQ	108.4	9.1	
Number on serotonin-reuptake inhibitor	13		
Number with psychiatric comorbidities	29		
Number without psychiatric comorbidities	13		
YBOCS total pre-CBT	24.6	4.7	
YBOCS total post-CBT	15.0	5.3	<0.001*
YBOCS obsessions (1–5) pre-CBT	12.0	2.7	
YBOCS obsessions (1–5) post-CBT	7.9	3.1	<0.001*
YBOCS compulsions (6–10) pre-CBT	12.6	2.3	
YBOCS compulsions (6–10) post-CBT	7.1	2.7	<0.001*
HAMA pre-CBT	12.5	5.3	
HAMA post-CBT	8.5	5.1	<0.001*
MADRS pre-CBT	15.6	9.3	
MADRS post-CBT	11.0	8.9	<0.001*
GAS pre-CBT	57.7	8.6	
GAS post-CBT	69.5	13.4	<0.001*

*Paired t test, comparing pre- versus post-CBT.

Table 2. Associations between predicted and actual post-CBT OCD symptom severity for eight functional brain connectivity networks subjected to multivariate analysis

Network	R^2
Default mode	0.672*
Visual	0.505*
Dorsal attention	0.022
Somatosensory motor	0.123
Cinguloopercular	0.170
Frontoparietal	0.215
Subcortical	0.148
Ventral attention	0.057

* $p \leq 0.006$; Bonferroni-corrected significance level.

power in both the DMN ($R^2 = 0.67$ with vs. $R^2 = 0.69$ without) and visual network ($R^2 = 0.51$ with vs. $R^2 = 0.53$ without). No feature sets accounted for significant variance in participants' postwaitlist YBOCS scores, indicating that prediction of OCD outcome was specifically related to CBT as opposed to the mere passage of time. To confirm that results were specific to predicting OCD symptom outcomes, we also conducted cross-validations for the HAMA and MADRS scores both before and after treatment. No networks accounted for significant variance in these end points. To confirm that our results were specific to OCD outcome and not comorbid conditions such as depression and anxiety, we used the pretreatment data in two SVM cross-validations to predict whether a participant had (*i*) a depressive disorder ($n = 10$; major depressive disorder, dysthymic disorder, and depressive disorder not otherwise specified) and/or (*ii*) an anxiety disorder ($n = 24$; generalized anxiety disorder, social anxiety disorder, panic disorder, posttraumatic stress disorder, specific phobia, and body dysmorphic disorder). See *SI Methods* for more information. No feature sets had a classification accuracy (averaged over 10 iterations) that was statistically different from chance (50%) in either cross-validation.

We also performed an SVM cross-validation to determine if pretreatment FC feature sets from the DMN and visual network could classify significant clinical change (responders) according to previously published expert consensus criteria (YBOCS decrease of $\geq 35\%$ and CGI-I of 1 or 2) (51). Both networks were able to classify responders ($n = 23$) from nonresponders with high accuracy (visual network accuracy = 70.0%, $P < 0.001$; DMN accuracy = 67.9% accuracy, $P < 0.001$; chance = 50%).

To establish that results were specific to predicting treatment response rather than merely reflecting OCD symptom severity, we examined post hoc the predictive power of pretreatment connectivity on pretreatment YBOCS scores. Neither the visual network nor the DMN (the networks whose pretreatment FC significantly accounted for variance in posttreatment YBOCS) accounted for significant variance in pretreatment YBOCS when using pretreatment FC feature sets. We also examined relationships between posttreatment feature sets and posttreatment YBOCS. Only the posttreatment visual network feature set that also included the amygdala ROIs could predict posttreatment YBOCS ($R^2 = 0.24$, RMSE = 4.6; $P < 0.001$) (Figs. S2 and S3 and see *Supporting Information* for additional post hoc analyses).

Discussion

This OCD study uses multivariate pattern recognition to identify neurobiological predictors of treatment response. Pretreatment multivariate connectivity in the DMN and the visual network significantly predicted individual patients' OCD symptoms after 4 wk of intensive CBT. Conversely, pretreatment OCD symptom severity was only moderately associated with posttreatment severity and, along with medication status, was not ranked in the

top quartile of feature predictive strength. Furthermore, these clinical variables were not able to reliably predict posttreatment YBOCS when used as features on their own in the cross-validation. Thus, brain connectivity far exceeded more readily obtained, a priori clinical information in its prognostic value for treatment response. These findings have implications for identifying who will benefit most from CBT, as well as for understanding the pathophysiology of OCD as it relates to CBT effects.

This predictive power of multivariate connectivity was validated in several ways (beyond our cross-validation procedure). First, it was specific to OCD symptoms and not to anxiety and depression. Second, it did not apply to cross-sectional pretreatment OCD symptoms. Third, changes predicted were specific to CBT and not merely a function of the passage of time. These results suggest that pretreatment connectivity reflects the capacity of an individual with OCD to return to normalcy—as quantified by YBOCS—after intensive CBT, independent of his/her starting symptom severity. Thereby, these connectivity patterns may reflect network plasticity and amenability to treatment-induced modulation. The SVM classification results that showed that both DMN and visual network pretreatment functional connectivity values could significantly predict responders vs. nonresponders adds further evidence to this narrative.

Pretreatment connectivity within the DMN was most predictive of end point OCD symptoms. This could reflect the potential of certain individuals' DMN to reorganize to provide a neural instantiation for modified behaviors taught during CBT. The DMN has been associated with self-referential processing (52), and obsessions often contain “evaluative dimensions about the self” (53). These may be associated with contamination-related compulsions (54) and possibly with an overinflated sense of personal responsibility (e.g., moral or religious scrupulosity) or obsessive concerns about harm. It is thus plausible that DMN connectivity patterns are related to OCD symptoms and/or responsiveness to CBT. Indeed, recent neuroimaging studies have found abnormal connectivity in the DMN and its constituent regions to be associated with OCD symptoms (17, 55). Given the proposed functions of the DMN, these studies suggest a possible contributor to self-oriented repetitive obsessions in some OCD patients: an impaired inability of the medial frontal cortex to evaluate performance (56, 57). For example, the hands are compulsively washed again because the first time was not “good enough,” or prayer is scrupulously repeated since it was not sufficiently “pure” or “devout” the first time. Our results could reflect the potential for the DMN to adjust toward a more adaptive state, allowing one's thoughts to escape the loop of self-referential processing and to switch to externally oriented, goal-directed cognition (58).

Pretreatment connectivity across the visual network also significantly predicted end point OCD symptoms. In anxiety

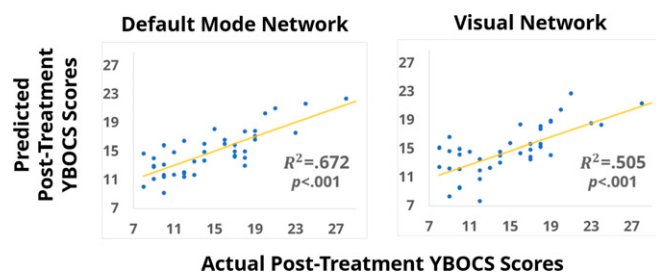


Fig. 2. Scatterplots depicting the relationship between the array of predicted posttreatment YBOCS values with the actual posttreatment YBOCS values when the LASSO cross-validation model was relying on feature sets that included pretreatment functional connectivity from the default mode network (Left) and the visual network (Right).

19. Stern ER, Fitzgerald KD, Welsh RC, Abelson JL, Taylor SF (2012) Resting-state functional connectivity between fronto-parietal and default mode networks in obsessive-compulsive disorder. *PLoS One* 7:e36356.
20. Hou J, et al. (2013) Morphologic and functional connectivity alterations of corticostriatal and default mode network in treatment-naïve patients with obsessive-compulsive disorder. *PLoS One* 8:e83931.
21. Göttlich M, Krämer UM, Kordon A, Hohagen F, Zurowski B (2014) Decreased limbic and increased fronto-parietal connectivity in unmedicated patients with obsessive-compulsive disorder. *Hum Brain Mapp* 35:5617–5632.
22. Maia TV, Cooney RE, Peterson BS (2008) The neural bases of obsessive-compulsive disorder in children and adults. *Dev Psychopathol* 20:1251–1283.
23. Menzies L, et al. (2008) Integrating evidence from neuroimaging and neuropsychological studies of obsessive-compulsive disorder: The orbitofronto-striatal model revisited. *Neurosci Biobehav Rev* 32:525–549.
24. Power JD, et al. (2011) Functional network organization of the human brain. *Neuron* 72:665–678.
25. Brem S, et al. (2012) Neuroimaging of cognitive brain function in paediatric obsessive compulsive disorder: A review of literature and preliminary meta-analysis. *J Neural Transm (Vienna)* 119:1425–1448.
26. Milad MR, Rauch SL (2012) Obsessive-compulsive disorder: Beyond segregated corticostriatal pathways. *Trends Cogn Sci* 16:43–51.
27. Stern ER, Taylor SF (2014) Cognitive neuroscience of obsessive-compulsive disorder. *Psychiatr Clin North Am* 37:337–352.
28. Szeszko PR, et al. (1999) Orbital frontal and amygdala volume reductions in obsessive-compulsive disorder. *Arch Gen Psychiatry* 56:913–919.
29. Szeszko PR, et al. (2004) Amygdala volume reductions in pediatric patients with obsessive-compulsive disorder treated with paroxetine: Preliminary findings. *Neuropsychopharmacology* 29:826–832.
30. Admon R, et al. (2012) Functional and structural neural indices of risk aversion in obsessive-compulsive disorder (OCD). *Psychiatry Res* 203:207–213.
31. de Vries FE, et al. (2014) Compensatory frontoparietal activity during working memory: An endophenotype of obsessive-compulsive disorder. *Biol Psychiatry* 76: 878–887.
32. van Velzen LS, et al. (2015) Altered inhibition-related frontolimbic connectivity in obsessive-compulsive disorder. *Hum Brain Mapp* 36:4064–4075.
33. DiNardo P, Brown T, Barlow D (1994) *Anxiety Disorders Interview Schedule for DSM-IV: Lifetime Version* (Graywind, Albany, NY).
34. Goodman WK, et al. (1989) The Yale-Brown obsessive compulsive scale. I. Development, use, and reliability. *Arch Gen Psychiatry* 46:1006–1011.
35. Hamilton M (1959) The assessment of anxiety states by rating. *Br J Med Psychol* 32: 50–55.
36. Montgomery SA, Asberg M (1979) A new depression scale designed to be sensitive to change. *Br J Psychiatry* 134:382–389.
37. Endicott J, Spitzer RL, Fleiss JL, Cohen J (1976) The global assessment scale. A procedure for measuring overall severity of psychiatric disturbance. *Arch Gen Psychiatry* 33:766–771.
38. Kozak MJ, Foa EB (1997) *Mastery of Obsessive-Compulsive Disorder: A Cognitive-Behavioral Approach Client Workbook* (Oxford Univ Press, New York).
39. Power JD, Barnes KA, Snyder AZ, Schlaggar BL, Petersen SE (2012) Spurious but systematic correlations in functional connectivity MRI networks arise from subject motion. *Neuroimage* 59:2142–2154.
40. Power JD, et al. (2014) Methods to detect, characterize, and remove motion artifact in resting state fMRI. *Neuroimage* 84:320–341.
41. Harrison BJ, et al. (2009) Altered corticostriatal functional connectivity in obsessive-compulsive disorder. *Arch Gen Psychiatry* 66:1189–1200.
42. Mataix-Cols D, et al. (2004) Distinct neural correlates of washing, checking, and hoarding symptom dimensions in obsessive-compulsive disorder. *Arch Gen Psychiatry* 61:564–576.
43. Jung WH, et al. (2009) BOLD response during visual perception of biological motion in obsessive-compulsive disorder: An fMRI study using the dynamic point-light animation paradigm. *Eur Arch Psychiatry Clin Neurosci* 259:46–54.
44. Stern ER (2014) Neural circuitry of interoception: New insights into anxiety and obsessive-compulsive disorders. *Curr Treat Options Psychiatry* 1:235–247.
45. Hou J-M, et al. (2014) Resting-state functional connectivity abnormalities in patients with obsessive-compulsive disorder and their healthy first-degree relatives. *J Psychiatry Neurosci* 39:304–311.
46. Tibshirani R (1996) Regression shrinkage and selection via the lasso. *J R Stat Soc Ser B Stat Methodol* 58:267–288.
47. Efron B, Hastie T, Johnstone I, Tibshirani R (2004) Least angle regression. *Ann Stat* 32: 407–499.
48. Chong I-G, Jun C-H (2005) Performance of some variable selection methods when multicollinearity is present. *Chemom Intell Lab Syst* 78:103–112.
49. Pereira F, Mitchell T, Botvinick M (2009) Machine learning classifiers and fMRI: A tutorial overview. *Neuroimage* 45(Suppl 1):S199–S209.
50. American Psychiatric Association (1994) *Diagnostic and Statistical Manual of Mental Disorders* (Am Psychiatr Assoc, Washington, DC), 4th Ed.
51. Mataix-Cols D, et al. (2016) Towards an international expert consensus for defining treatment response, remission, recovery and relapse in obsessive-compulsive disorder. *World Psychiatry* 15:80–81.
52. Sheline YI, et al. (2009) The default mode network and self-referential processes in depression. *Proc Natl Acad Sci USA* 106:1942–1947.
53. Aardema F, et al. (2013) Fear of self and obsessiveness: Development and validation of the fear of self questionnaire. *J Obsessive Compuls Relat Disord* 2:306–315.
54. Doron G, Sar-El D, Mikulincer M (2012) Threats to moral self-perceptions trigger obsessive compulsive contamination-related behavioral tendencies. *J Behav Ther Exp Psychiatry* 43:884–890.
55. Peng ZW, et al. (2014) Default network connectivity as a vulnerability marker for obsessive compulsive disorder. *Psychol Med* 44:1475–1484.
56. Schwartz JM (1999) A role for volition and attention in the generation of new brain circuitry: Toward a neurobiology of mental force. *J Conscious Stud* 6:115–142.
57. Szechtman H, Woody E (2004) Obsessive-compulsive disorder as a disturbance of security motivation. *Psychol Rev* 111:111–127.
58. Anticevic A, et al. (2012) The role of default network deactivation in cognition and disease. *Trends Cogn Sci* 16:584–592.
59. Doehrmann O, et al. (2013) Predicting treatment response in social anxiety disorder from functional magnetic resonance imaging. *JAMA Psychiatry* 70:87–97.
60. Whitfield-Gabrieli S, et al. (2016) Brain connectomics predict response to treatment in social anxiety disorder. *Mol Psychiatry* 21:680–685.
61. Bohon C, Hembacher E, Moller H, Moody TD, Feusner JD (2012) Nonlinear relationships between anxiety and visual processing of own and others' faces in body dysmorphic disorder. *Psychiatry Res* 204:132–139.
62. Foa EB, Kozak MJ (1986) Emotional processing of fear: Exposure to corrective information. *Psychol Bull* 99:20–35.
63. Craske MG, et al. (2008) Optimizing inhibitory learning during exposure therapy. *Behav Res Ther* 46:5–27.
64. Lang PJ, et al. (1998) Emotional arousal and activation of the visual cortex: An fMRI analysis. *Psychophysiology* 35:199–210.
65. Pizzagalli DA, et al. (2002) Affective judgments of faces modulate early activity (approximately 160 ms) within the fusiform gyri. *Neuroimage* 16:663–677.
66. Vuilleumier P, Richardson MP, Armony JL, Driver J, Dolan RJ (2004) Distant influences of amygdala lesion on visual cortical activation during emotional face processing. *Nat Neurosci* 7:1271–1278.
67. Vuilleumier P, Schwartz S (2001) Emotional facial expressions capture attention. *Neurology* 56:153–158.
68. Duncan S, Barrett LF (2007) The role of the amygdala in visual awareness. *Trends Cogn Sci* 11:190–192.
69. Fox E, et al. (2000) Facial expressions of emotion: Are angry faces detected more efficiently? *Cogn Emotion* 14:61–92.
70. Yovel I, Revelle W, Mineka S (2005) Who sees trees before forest? The obsessive-compulsive style of visual attention. *Psychol Sci* 16:123–129.
71. Pessoa L, Japee S, Sturman D, Ungerleider LG (2006) Target visibility and visual awareness modulate amygdala responses to fearful faces. *Cereb Cortex* 16:366–375.